ORGANOMETALLICS

pubs.acs.org/Organometallics Article

# Synthesis of Pyridines, Quinolines, and Pyrimidines via Acceptorless Dehydrogenative Coupling Catalyzed by a Simple Bidentate *P^N* Ligand Supported Ru Complex

Rajarshi Mondal and David E. Herbert*

Cite This: https://dx.doi.org/10.1021/acs.organomet.0c00058 Read Online

ACCESS | Metrics & More | Article Recommendations | Supporting Information

**ABSTRACT:** A ruthenium hydrido chloride complex (**1**) supported by a simple, heteroleptic bidentate *P^N* ligand (**L1**) containing a diarylphosphine and a benzannulated phenanthridine donor arm is reported. In the presence of base, complex **1** catalyzes multicomponent reactions using alcohol precursors to produce structurally diverse molecules including pyridines, quinolines, and pyrimidines via acceptorless dehydrogenative coupling pathways. Notably, **L1** does not bear readily (de)protonated Brønsted acidic or basic groups common to transition metal catalysts capable of these sorts of transformations, suggesting metal−ligand cooperativity does not play a significant role in the catalytic reactivity of **1**. A rare example of an $\eta^2$-aldehyde adduct of ruthenium was isolated and structurally characterized, and its role in acceptorless dehydrogenative coupling reactions is discussed.

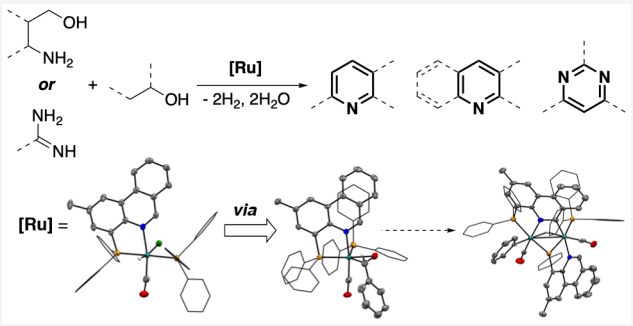




## INTRODUCTION

The Friedländer annulation reaction, in which 2-aminophenyl ketones or aldehydes are coupled with carbonyl compounds possessing acidic $\alpha$-hydrogens, is a straightforward approach to the preparation of substituted quinolines.[1] This atom-efficient reaction was made even more so with the discovery that the corresponding saturated alcohols could be used, provided they could be efficiently dehydrogenated *in situ.* The resulting "indirect" Friedländer annulation employs a single catalyst for both the oxidation of alcohols and their catalytic condensation.[2] The combination of the acceptorless dehydrogenation of alcohols with C−N bond-forming condensation reactions can in fact enable atom-efficient, one-pot, acceptorless dehydrogenative coupling (ADC) syntheses of a range of value-added organic molecules including *N*-heterocyclic pyridines, quinolines, pyrroles, and pyrimidines.[3] These can be mediated by a wide variety of mid to late transition metal complexes based on Ru,[4−10] Mn,[11−14] Ir,[15−17] Co,[18−20] and Ni.[21,22] With respect to catalytic efficiency, Ru precatalysts at present enable the highest reported yields at the lowest catalyst loadings. For example, Liu and Sun and co-workers reported efficient catalysis using loadings of 0.025 mol %, though relatively long reaction times (72 h) were required for high conversion.[6] In general, the most highly active Ru catalysts are comprised of tridentate, pincer-type ligands (Figure 1) typically bearing N−H[4−6] or O−H[7,23] moieties that lead to invocations of metal−ligand cooperativity (MLC).[24]

Given the recent debate over the activation of ligand-based N−H groups in related dehydrogenative amide synthesis[25,26] and reports that commercially available *cis*-(dimethyl sulfoxide)$_4$RuCl$_2$[2,27] and (PPh$_3$)$_3$RuCl$_2$[28] can catalyze the dehydrogenative/dehydrative formation of polysubstituted quinolines from 2-aminobenzyl alcohol and primary or secondary alcohols in respectable yields in the presence of a significant excess of a sacrificial hydrogen acceptor, we were curious as to the capability of complexes supported by simpler ligand frameworks lacking reactive E−H groups or obvious Brønsted basic sites to carry out complex, multicomponent Friedländer-type ADC reactions. Catalyst platforms based on simple, bidentate ligands that can facilitate ADC reactions with a wide product scope would expand the chemical space available for ligand design for these useful reactions.

We have been exploring the utility of bidentate *P^N* coordinating ligands combining phosphine and phenanthridine (3,4-benzoquinoline) donors,[29] that are benzannulated analogues of (8-diphenylphosphino)quinoline.[30] Using phenanthridine in place of quinoline opens up a more easily accessed range of *N*-heterocycle substituted *P^N* proligands as 2-substituted phenanthridines can be assembled using one-pot cross-coupling/condensation reactions[31,32] that are more convenient compared with less tractable Skraup conditions

Received: January 27, 2020




https://dx.doi.org/10.1021/acs.organomet.0c00058
Organometallics XXXX, XXX, XXX−XXX

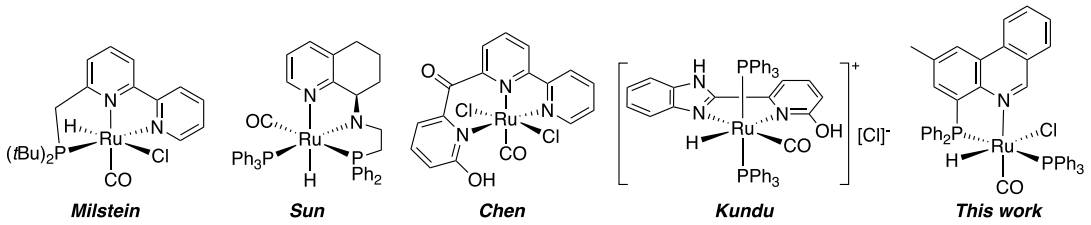


**Figure 1.** Representative structures of highly active Ru catalysts for ADC reactions.

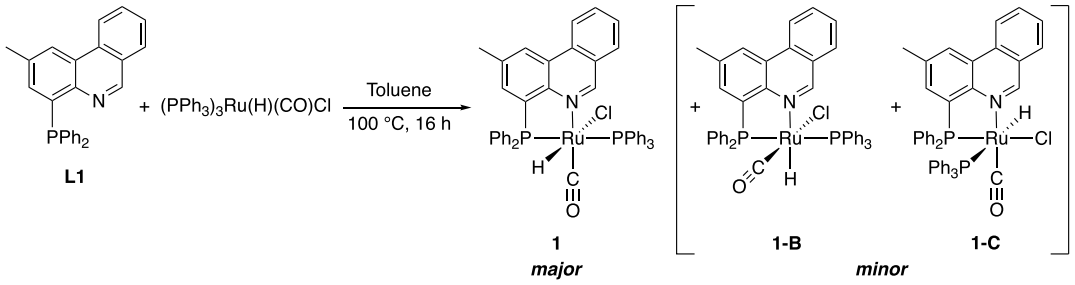


**Figure 2.** Synthesis of precatalyst **1** and accompanying minor isomers.

required for synthesis of 6-substituted quinolines.[33] Here, we report that a simple octahedral Ru complex (**1**) supported by this type of ligand framework can catalyze ADC reactions in the presence of base to form substituted pyridines, quinolines, and pyrimidines at low loadings. While a number of systems for formation of polysubstituted pyridines and quinolines via ADC have been reported, the literature contains comparably fewer examples of the construction of pyrimidines, which find use in antibacterials, as pharmaceutical building blocks, and as photoemissive materials.[11,16,34,35] Importantly, **L1** does not contain obvious Brønsted acidic or basic sites, precluding MLC pathways.

## RESULTS AND DISCUSSION

**Catalyst Synthesis.** 4-(Diphenylphosphino)-2-methylphenanthridine (**L1**) was assembled from 4-bromo-2-methylphenanthridine and $Ph_2PCl$, as previously described.[32] The proligand **L1** was then reacted with $(PPh_3)_3RuH(CO)Cl$[36] in toluene at 100 °C for 16 h to give the target complex (**L1**)$(PPh_3)RuH(CO)Cl$ (**1**; Figure 2). Complex **1** precipitates from the reaction mixture as a fine yellow crystalline powder that is sparingly soluble in toluene but readily soluble in chlorinated and more polar solvents. $^{31}P\{^1H\}$ NMR spectroscopy confirmed installation of 1 equiv of the bidentate ligand and retention of a $PPh_3$ donor *trans* to the phosphorus arm of **L1** through the appearance of two doublets with a large coupling constant ($\delta_P$ = 57.71, 37.38; $^2J_{PP}$ = 285.5 Hz). The carbonyl and hydride ligands are also retained, with IR signatures of $\nu_{C\equiv O}$ = 1919 $cm^{-1}$ (vs) and $\nu_{Ru-H}$ = 1992 $cm^{-1}$ (w). The observed $\nu$(Ru—H) absorption fits into a trend with (L)$(PPh_3)_2RuH(CO)Cl$ (L = pyridine, isoquinoline), whereby benzannulation of the heterocyclic donor leads to a shift of $\nu$(Ru—H) to lower wavenumbers from 2008 $cm^{-1}$ for (pyridine)$(PPh_3)_2RuH(CO)Cl$[37] to 2000 $cm^{-1}$ for (isoquinoline)$(PPh_3)_2RuH(CO)Cl$[38] to 1992 $cm^{-1}$ for **1**. The hydride ligand is also visible in the $^1H$ NMR spectrum as an upfield-shifted pseudo triplet with similar coupling to both phosphine nuclei, suggesting a *cis* orientation. The NMR data again fits into a series with (L)$(PPh_3)_2RuH(CO)Cl$ (L = pyridine, isoquinoline); benzannulation is accompanied by a slight upfield shift of $\delta$(H) = −13.52 (L = pyridine; t, $^2J_{HP}$ = 19.5 Hz),[37] −13.39 (L = isoquinoline; t, $^2J_{HP}$ = 19.5 Hz),[38] and −13.20 (**1**; pseudo t, $^2J_{HP}$ = 21.8 Hz).

Also present in solution are two minor isomers, which could not be separated by crystallization. The hydride resonances of the minor isomers are instructive as to their structures. In the more prominent minor isomer (**1-B**: −12.27 ppm; dd, $^2J_{PH}$ = 26.0, 15.0 Hz), the hydride couples differently to each phosphorus but with the magnitude of the coupling constants consistent with a similar *cis* orientation of the hydride and two phosphines to the major isomer. In the $^{31}P\{^1H\}$ NMR spectrum, signals attributed to **1-B** appear as a set of doublets (46.92 and 40.64 ppm; $^2J_{PP}$ = 310.7 Hz) with similarly large $^2J_{PP}$ as seen for the major isomer, suggestive of a *trans* orientation to the phosphorus nuclei. These similarities lead us to favor a structural assignment for **1-B** where the two ligands of strongest *trans* influence (hydride and carbonyl) switch positions with respect to being *trans* to either the chloride or the phenanthridinyl nitrogen. The other minor isomer (**1-C**) does not show strong P—P coupling (signals at 78.0 and 28.8 ppm) and so likely has a *cis* orientation of the two phosphorus nuclei, with the $PPh_3$ *trans*-disposed to the hydride (**1-C**: −6.54 ppm; dd, $^2J_{PH}$ = 121.6, 27.0 Hz). The large change in $\delta_P$ observed for the diphenylphosphino unit of the *P^N* ligand is attributed to twisting of the ligand arm due to changes in the coordination sphere around the metal.[39] As it is not part of a chelate, the geometry of the $PPh_3$ ligand, and therefore $\delta_P$, is not impacted as significantly by changes in molecular structure. High-resolution mass spectrometry (HR-MS) and elemental analysis both indicate a pure mixture of isomers, so we refer here on in to this mixture in terms of the major isomer (**1**).

**Reactivity Studies.** To investigate the activity of **1** with respect to dehydrogenation of saturated alcohols, a toluene solution containing an excess of benzyl alcohol was combined with **1** and a base (KO*t*Bu) at ambient temperature and stirred for 2 h, forming a deep red solution. Neither liberated $H_2$ gas nor significant consumption of benzaldehyde were detected in $^1H$ NMR spectra of aliquots taken from the reaction mixture; however, dark red crystals of a benzaldehyde adduct (**2**) were isolated in substantial yield (64%) by layering the reaction


https://dx.doi.org/10.1021/acs.organomet.0c00058
Organometallics XXXX, XXX, XXX−XXX

mixture with pentane. Thus, while **1** appears to dehydrogenate benzyl alcohol, the resultant adduct does not easily liberate benzaldehyde, preventing turnover. Complex **2** is also formed, albeit in lower yields, by reaction of **1** with stoichiometric amounts of benzyl alcohol and base (Figure 3). Crystalline **2** is

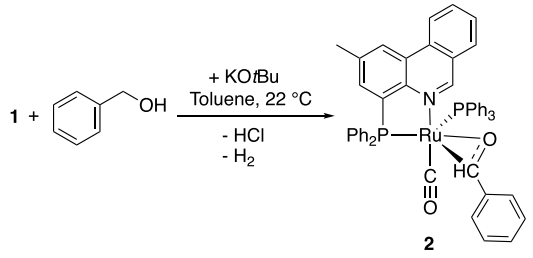


**Figure 3.** Dehydrogenation of benzyl alcohol and formation of **2**.

only sparingly soluble in toluene or benzene and does appear to liberate benzaldehyde upon heating or sonication, instead decomposing to unidentified metal-containing products.

Despite the numerous reports of Ru-based alcohol dehydrogenation catalysis, isolated Ru $\eta^2$-adducts of benzaldehyde turned out to be quite rare. To our knowledge, only two such complexes have been crystallographically characterized and solution characterization data was not delineated.[40,41] Complex **2** proved stable/soluble enough to obtain both solution and solid-state structural information. In solution, the metal-bound aldehyde C*H* resonates considerably upfield and shows coupling to both phosphines ($\delta_H$: 4.52 ppm; virtual triplet, $J_{PH}$ = 5 Hz) consistent with significant back-bonding from the metal. The $^{31}P\{^1H\}$ resonances of **2** appeared as a set of doublets (68.12 and 37.50 ppm; $J_{PP}$ = 38.38 Hz) with a smaller $J_{PP}$ coupling constant indicating a *cis* arrangement of the two phosphorus nuclei. Both the carbonyl and benzaldehyde group frequencies are observed by FT-IR spectroscopy, with absorptions assigned to $\nu_{C\equiv O}$ = 1896 cm$^{-1}$ (vs) and $\nu_{Ru—benzaldehyde}$ = 1584 cm$^{-1}$ (m). The carbonyl stretching frequency is only slightly lower than that in **1**, while the $\eta_2$-benzaldehyde stretch is significantly lower than that of the free organic molecule.

Single crystals suitable for crystallographic analysis could be grown for both **1** and **2** (Figure 4). For **1**, this enabled confirmation of the geometry of the major isomer as assigned by multinuclear NMR, with a hydride *trans* to a chloride. The solid-state structure of **2** is best described as having a Ru(0) sitting within a distorted trigonal bipyramid, with an $\eta^2$-aldehyde and two phosphines occupying the equatorial plane, and a carbonyl and phenanthridinyl nitrogen in axial positions. The elongation of the aldehyde C═O bond [C45−O1 1.344(5) Å] is consistent with stabilization of the low valent Ru center through significant $\pi$ back-bonding; the C═O distance is longer than that in the most closely related structurally characterized Ru−$\eta^2$-aldehyde complex, [Ru($\eta^2$-O═CHPh)(trop$_2$dae), trop$_2$dae = *N*,*N*′-bis(5*H*-dibenzo[*a*,*d*]-cycloheptene(5-yl)-1,4-diaminoethane); $d$($\eta^2$-C═O): 1.310(9) Å], which furthermore lacks an additional $\pi$-acidic CO ligand and whose precursor K[Ru(H)(trop$_2$dae)] is a potent precatalyst for the production of $H_2$ from alcohols in the presence of water.[41] The enhanced back-bonding and accompanying stability may speak to the reluctance of **2** to turn over following dehydrogenation of 1 equiv of primary alcohol.

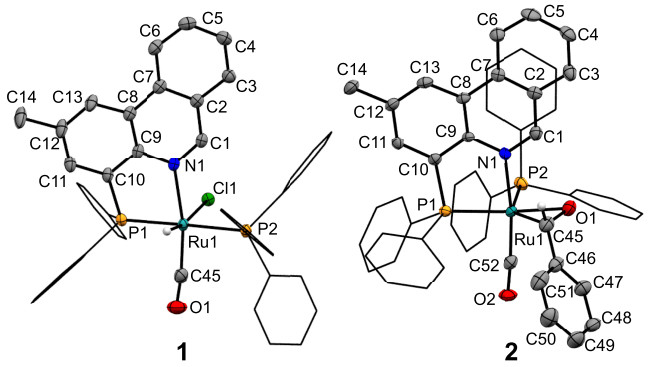


**Figure 4.** Solid-state structures of **1** and **2** with ellipsoids shown at 50% probability levels. With the exception of the hydride in **1** and aldehyde proton in **2**, hydrogen atoms and select atom labels are omitted for clarity. Selected bond distances (Å) and angles (deg): **1**: Ru1−P1 2.2812(6), Ru1−P2 2.4116(6), Ru1−N1 2.1966(19), Ru1−Cl1 2.5455(6), Ru1−C45 1.831(3), C45−O1 1.161(3); P1−Ru1−P2 169.51(2), P1−Ru1−Cl1 96.17(2), P2−Ru1−C1l 93.94(2), P1−Ru1−C45 89.23(8), P2−Ru1−C45 91.87(8), C45−Ru1−Cl1 99.32(8). **2**: Ru1−P1 2.2668(11), Ru1−P2 2.3899(11), Ru1−N1 2.164(3), Ru1−O1 2.104(3), Ru1−C45 2.136(4), Ru1−C52 1.822(4), C45−O1 1.344(5), C52−O2 1.175(5); P1−Ru1−P2 102.95(4), P1−Ru1−C52 91.40(13), P2−Ru1−C52 95.47(14), N1−Ru1−P1 81.28(9), C45−Ru1−P1 118.58(13), C45−Ru1−N1 85.80(15), C45−O1−Ru1 72.8(2), O1−Ru1−C45 36.94(14), C52−Ru1−N1 171.43(16), C52−Ru1−O1 100.29(16).

Considering that **1** can mediate the dehydrogenation of benzyl alcohol in the presence of exogenous base but is reluctant to dissociate the generated benzaldehyde, we proceeded to investigate the dehydrogenation of a secondary alcohol to see if increased steric bulk could promote dissociation of the oxidized product. Complex **1** proved still sluggish in the acceptorless dehydrogenation of cyclohexanol. Only ∼5% conversion to cyclohexanone was observed by $^1H$ NMR after 24 h reaction time in a capped vial at room temperature using 0.33 mol % catalyst loading. In an open reflux, activity is moderately boosted to 18% conversion. The fate of **1** proved more interesting. Isolation and recrystallization of the organometallic product (**3**) from the reaction mixtures gave orange crystals in ∼20% yield based on Ru, on average. The $^{31}P\{^1H\}$ NMR spectrum contained three coupled resonances. Two of these resonances are consistent with retention of a *P*^*N* ligand (64.9 ppm; d, $J_{PP}$ = 258 Hz) and a PPh$_3$ (32.4 ppm; d, $J_{PP}$ = 160 Hz), though the coupling constants make it clear these two nuclei do not couple to each other. The third resonance appeared considerably downfield, with a chemical shift more consistent with a bridging phosphide (111.5 ppm; dd, $J_{PP}$ = 258, 160 Hz). In the hydride region of the $^1H$ NMR spectrum, the hydride resonances of **1** have been replaced with a triplet of doublets (−8.24 ppm; $^2J_{HP}$ = 18.5, 6.8 Hz). X-ray crystallographic analysis of **3** (Figure 5) revealed the formation of a binuclear dimer, where two Ru centers are bridged by a hydride, a phosphide, and an imide derived from P−C and C−H activation of two *P*^*N* ligands.

Activation of a diphenylphosphino P−C unit with insertion of Ru into a P−Ph bond appears to have led to phenyl group transfer, while C−H activation at the 6-position of a phenanthridine ligand arm forms an unusual $\kappa^2$-Ru$_1$, $\mu^2$-Ru$_1$,Ru$_2$ arrangement supporting the Ru−Ru unit (Figure 6). Formation of a related dimer via P−C bond cleavage and


https://dx.doi.org/10.1021/acs.organomet.0c00058
*Organometallics* XXXX, XXX, XXX−XXX

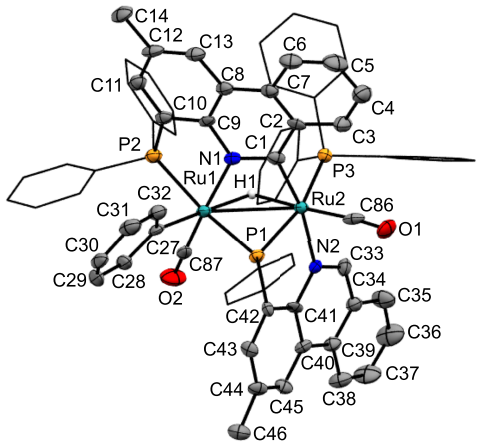


**Figure 5.** Solid-state structure of **3** with ellipsoids shown at 50% probability levels. Select hydrogen atoms and atom labels omitted for clarity. Selected bond distances (Å) and angles (deg): C(1)−Ru(2) 2.075(6), C(27)−Ru(1) 2.127(6), C(86)−Ru(2) 1.859(8), C(87)−Ru(1) 1.835(7), N(1)−Ru(1) 2.115(5), N(2)−Ru(2) 2.216(5), P(1)−Ru(2) 2.2749(18), P(1)−Ru(1) 2.3350(19), P(2)−Ru(1) 2.3115(19), P(3)−Ru(2) 2.408(2), Ru(1)−Ru(2) 2.9570(13), Ru(1)−H(1) 1.83(5), Ru(2)−H(1) 1.79(5); N(1)−C(1)−Ru(2) 109.0(4), C(2)−C(1)−Ru(2) 133.2(5), C(32)−C(27)−Ru(1) 121.9(5), C(28)−C(27)−Ru(1) 123.0(5), O(1)−C(86)−Ru(2) 175.0(5), O(2)−C(87)−Ru(1) 175.8(6), C(1)−N(1)−Ru(1) 116.5(4), C(9)−N(1)−Ru(1) 120.9(4), C(33)−N(2)−Ru(2) 123.8(4), C(41)−N(2)−Ru(2) 118.7(4), Ru(2)−P(1)−Ru(1) 79.79(6), C(15)−P(2)−Ru(1) 117.3(2), C(10)−P(2)−Ru(1) 101.0(2), N(1)−Ru(1)−P(1) 86.50(14), P(2)−Ru(1)−P(1) 164.46(6), P(2)−Ru(1)−Ru(2) 128.80(5), P(1)−Ru(1)−Ru(2) 49.21(5), N(1)−Ru(1)−Ru(2) 64.66(14), Ru(2)−Ru(1)−H(1) 34.6(16), P(1)−Ru(1)−H(1) 80.9(16), N(1)−Ru(1)−H(1) 74.4(15), Ru(1)−Ru(2)−H(1) 35.5(16), P(1)−Ru(2)−H(1) 83.4(16).

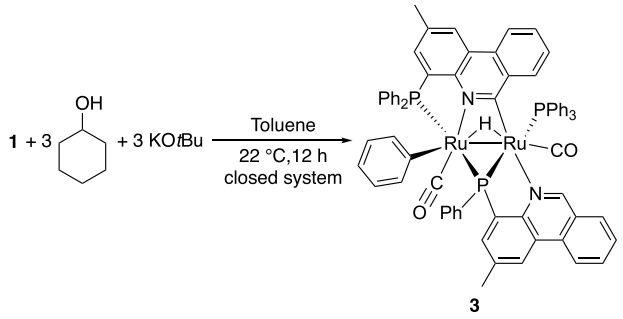


**Figure 6.** Decomposition of **1** leading to formation of **3**.

phenyl group transfer was observed on treatment of the commercially available precatalyst $Ru(HN(CH_2CH_2PPh_2)_2)$-$H(Cl)(CO)$ with base at room temperature, along with a number of other products.[42]

The finding that **1** can mediate alcohol dehydrogenation but is reluctant to liberate the resulting aldehyde leading to a stable aldehyde adduct (**2**) or decomposition (formation of **3**) led us to investigate if the unsaturated organic fragment could be intercepted by an incoming nucleophile. Optimization of ADC catalysis conditions was carried out using the reaction of 2-aminobenzyl alcohol and 1-phenylethanol (Table 1). We first confirmed that no reaction was observed when either catalyst or base is absent (runs 1 and 2); an unidentified side product was observed in the presence of base alone but with no consumption of alcohol. We note moderate conversion (34%) when the simple $(PPh_3)_3Ru(CO)(Cl)H$ is used in place of **1** (run 4). Under the same conditions using complex **1**, the yield of product is boosted to 54% (run 3). A decrease in isolated yield is observed when the reaction is performed in a more polar solvent such as dioxane or THF (runs 5 and 6). Using KOH in place of an alkoxide base did not substantially affect the observed yield (runs 7 and 13). We were able to decrease the catalyst loading to 0.1 mol % with 0.5 equiv of base without impacting the yield (run 8), while decreasing the excess of secondary alcohol led to a drop in yield (run 9). In fact, higher yields could be obtained at 0.025 mol % catalyst loading, provided an excess (2 equiv) of KO*t*Bu base and secondary alcohol was used (run 10). No significant improvement was observed on extending the reaction time from 24 to 48 h (run 11). While even lower catalyst loadings of 0.01 mol % (run 12) led to respectable isolated yields, run 10 (bold in Table 1) represents our optimized reaction conditions. Interestingly, both the $\eta^2$-aldehyde adduct **2** and hydride-bridged dimer **3** are competent precatalysts for this ADC reaction as well (runs 14−17). The presence of an exogenous nucleophile, in this case aminobenzyl alcohol, therefore appears to be sufficient to turn over **2**. In addition, formation of **3** is not a catalytic dead-end.

The scope of catalytic ADC of γ-amino alcohols and secondary alcohols was then explored, and the results are shown in Table 2. Isolated yields >80% were obtained for a range of substrate combinations. Overall, catalytic coupling using **1** is tolerant of a variety of chloro, methoxy, and aryl substituents, and a range of aliphatic ring sizes, with highest yields observed for the highest boiling point secondary alcohols presumably as a result of minimal losses during open reflux. In some cases where low yields were observed (**4b**), increasing the amount of base used led to a significant boost in yield. In this way, we were able to prepare a variety of substituted pyridines and quinolines, including novel compounds such as 2-(8-methoxynaphthyl)-6-phenylpyridine (**4k**). Catalyst loadings as low as 0.025 mol % still allowed for isolation of appreciable amounts of product, in some cases with yields exceeding 80% (**4f**, **4n**, and **4t**). In comparison, Ru complexes of tridentate amido ligands can reach similar yields for this reaction only with extended reaction times of 72 h at comparable catalyst loadings.[6] To probe the mechanism of ADC, an aliquot of the reaction mixture from the synthesis of 2-methyl-5,6,7,8-tetrahydroquinoline (**4r**) from cyclohexanol and 3-amino-1-butanol was analyzed midway through the reaction at the 12 h mark (see the Supporting Information, Figures S18 and S98). In addition to cyclohexanone (observed by $^1$H NMR) and the product (**4r**), a number of peaks consistent with chemical species that plausibly form as intermediates could be discerned by mass spectrometry including the direct product of dehydrative coupling of 3-amino-1-butanol and cyclohexanone, 2,3,5,6,7,8-hexahydro-2-methyl-4(1*H*)-quinolinone, and 2,3,5,6,7,8-hexahydroquinoline (Figure S18). Formation of these species is consistent with the mechanism proposed by Pan et al. based on DFT-calculated relative free energies of the likely organic intermediates.[6]

The utility of **1** in catalytic ADC coupling reactions of γ-amino alcohols and secondary alcohols led us to next explore one-pot, three-component pyrimidine syntheses from benzamidines, a primary alcohol, and a secondary alcohol (Table 3). In these reactions, an extra equivalent of base was introduced


https://dx.doi.org/10.1021/acs.organomet.0c00058
Organometallics XXXX, XXX, XXX−XXX

**Table 1. Optimization of Reaction Conditions for 2-Phenylquinoline Synthesis Using 1**

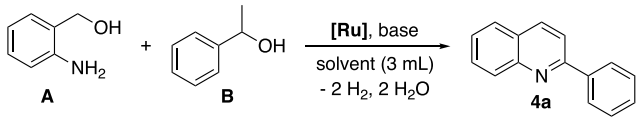


| run | A:B | equiv. base | [Ru] (mol %) | solvent | $T^a$ (°C) | $t$ (h) | yield$^c$ (%) |
|---|---|---|---|---|---|---|---|
| 1 | 1:2 | 0.5 (KO*t*Bu) | | toluene | 110 | 24 | 0 |
| 2 | 1:2 | | **1** (0.5) | toluene | 110 | 24 | 0 |
| 3 | 1:2 | 0.5 (KO*t*Bu) | **1** (0.5) | toluene | 110 | 24 | 54 |
| 4 | 1:2 | 0.5 (KO*t*Bu) | **1** (0.5)$^b$ | toluene | 110 | 24 | 34 |
| 5 | 1:2 | 0.5 (KO*t*Bu) | **1** (0.5) | dioxane | 101 | 24 | 45 |
| 6 | 1:2 | 0.5 (KO*t*Bu) | **1** (0.5) | THF | 66 | 24 | 14 |
| 7 | 1:2 | 0.5 (KOH) | **1** (0.5) | toluene | 110 | 24 | 38 |
| 8 | 1:2 | 0.5 (KO*t*Bu) | **1** (0.1) | toluene | 110 | 24 | 36 |
| 9 | 1:1 | 0.5 (KO*t*Bu) | **1** (0.1) | toluene | 110 | 24 | 46 |
| 10 | 1:2 | 2 (KO*t*Bu) | **1** (0.025) | toluene | 110 | 24 | 61 |
| 11 | 1:2 | 2 (KO*t*Bu) | **1** (0.025) | toluene | 110 | 48 | 66 |
| 12 | 1:2 | 2 (KO*t*Bu) | **1** (0.01) | toluene | 110 | 24 | 43 |
| 13 | 1:2 | 2 (KOH) | **1** (0.025) | toluene | 110 | 24 | 60 |
| 14 | 1:2 | 2 (KO*t*Bu) | **2** (1.0) | toluene | 110 | 24 | 74 |
| 15 | 1:2 | 2 (KO*t*Bu) | **2** (0.5) | toluene | 110 | 24 | 50 |
| 16 | 1:2 | 2 (KO*t*Bu) | **3** (0.5) | toluene | 110 | 24 | 77 |
| 17 | 1:2 | 2 (KO*t*Bu) | **3** (0.25) | toluene | 110 | 24 | 65 |

$^a$Conditions: open system under an Ar atmosphere, in a heating bath set to 20 °C above the solvent boiling point. $^b$$(PPh_3)_3Ru(CO)HCl$ used in place of **1**. $^c$Isolated yield.

**Table 2. Catalytic ADC of γ-Amino Alcohols and Secondary Alcohols**[a]

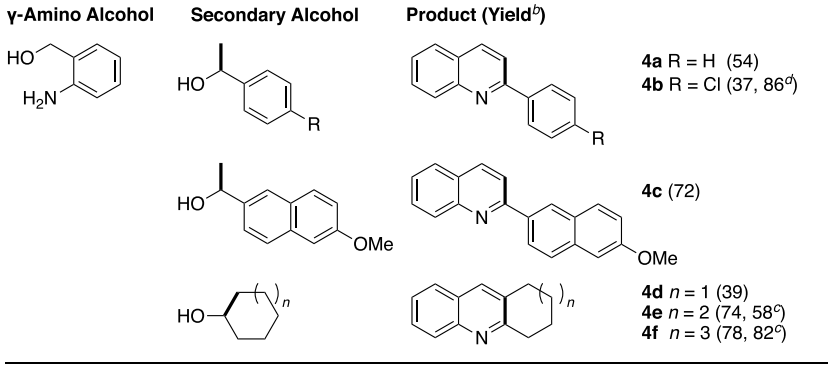


$^a$Reaction conditions: γ-amino alcohol (2 mmol), secondary alcohol (4 mmol), KO*t*Bu (1 mmol), **1** (0.5 mol %), toluene reflux, Ar atmosphere, open system, 24 h. $^b$Isolated yields following column chromatography, average of two trials. $^c$KO*t*Bu (4 mmol), **1** (0.025 mol %). $^d$KO*t*Bu (4 mmol), **1** (0.5 mol %).


https://dx.doi.org/10.1021/acs.organomet.0c00058
Organometallics XXXX, XXX, XXX−XXX

**Table 3. Catalytic ADC Synthesis of Pyrimidines Using Various Alcohols and Benzamidines**[a]

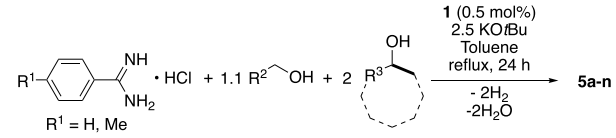


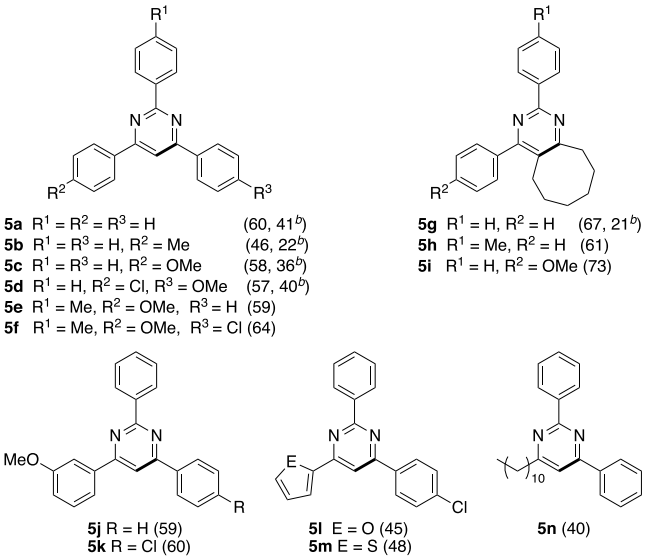


[a]Conditions unless otherwise specified: benzamidine·HCl (1 mmol), primary alcohol (1.1 mmol), secondary alcohol (2 mmol), KO*t*Bu (2.5 mmol), **1** (0.5 mol %), and 8 mL of toluene under an Ar atmosphere at open reflux. Isolated yields following column chromatography are shown in parentheses. [b]Benzamidine·HCl (1 mmol), primary alcohol (1.1 mmol), secondary alcohol (1.1 mmol), KO*t*Bu (3.5 mmol), **1** (0.025 mol %).

to enable use of the more easily handled hydrochloride salt of the benzamidine precursors. Pyrimidines **5a−n** could be obtained in respectable yields following column chromatography (40−73%) using a catalyst loading of 0.5 mol % (see the Supporting Information for optimization). In comparison, similar yields using Mn-based catalysts require higher catalyst loadings of 2[34] or 5 mol %,[11] as do supported Pt nanoparticles.[35] We also note that supported Ru nanoparticles are much less efficient at this transformation, with much lower conversions (∼25%) reported at higher catalyst loadings.[35] This supports homogeneous reactivity mediated by **1**. To our knowledge, only one other report of efficient, Ru-mediated homogeneous catalysis of pyrimidine formation from alcohols has appeared in the literature, and again invokes a key role for metal−ligand cooperativity.[23]

Lowering the catalyst loading to 0.025 mol % led to a reduction in the isolated yields, though appreciable conversion could still be observed in the presence of added base (Table 3, conditions *b*). The reaction conditions are similarly tolerant of electron-releasing or -withdrawing groups, alkane-derived primary alcohols, heteroatom-containing moieties such as furan (**5l**) and thiophene (**5m**), and the formation of fully substituted pyrimidines (**5g−i**) through the use of *β*-substituted secondary alcohols. Varying the electronics of the benzamidine by including an electron-releasing methyl group (**5e,f,h**) did not appreciably impact product yields.

Using a stoichiometric mixture of benzamidine (as hydrochloride salt), phenyl ethanol, and benzyl alcohol, pyrimidine **5a** formed in a 45% yield, with a mixture of the *β*-alkylated secondary alcohol (1,3-diphenylpropan-1-ol) and unreacted phenyl ethanol comprising the remainder of the isolated product. Under similar conditions but omitting the benzamidine, complete conversion to a 3:1 mixture of coupled products, 1,3-diphenylpropan-1-ol and the corresponding ketone 1,3-diphenylpropan-1-one, was found after 2.5 h. The unsaturated chalcone, proposed as a key intermediate in catalytic pyrimidine synthesis from alcohols,[23,35] was not observed. Subsequent addition of an equivalent of benzamidine to this reaction mixture and resubmission to the reaction conditions led to moderate conversion to **5a** (12%). The hydrogenation of chalcone and 1,3-diphenylpropan-1-one appears responsible for the diminished conversion to **5a**, likely a result of less efficient dehydrogenation of the coupled alcohols compared to the parent starting materials. In comparison, related Mn-based catalysts have been demonstrated to efficiently catalyze four-component reactions, where initial *β*-alkylation of secondary alcohols by primary alcohols can be followed by addition of another primary alcohol and an amidine to produce even more complex pyrimidines in a one-pot process.[34]

## CONCLUSION

In summary, a Ru complex (**1**) supported by a simple *P^N* ligand comprised of a benzannulated pyridine and a phosphine donor has proved efficient in a range of ADC-type reactions, enabling the catalytic synthesis of pyridines, quinolines, and pyrimidines at some of the lowest catalyst loadings reported.[6,23] With respect to ligand design, we note that the participation of the ligand (**L1**) in an active, cooperative fashion as proposed for a range of dehydrogenation-type reactivity[24] is unlikely in the case of **1**. As has been previously suggested for quinoline-derived *N^N^P* ligands,[6] the benzo-fused *π*-extended phenanthridine ring may provide added stability enabling the observed high catalytic efficiency. The sluggish turnover in dehydrogenation of alcohols in the absence of exogenous amines and the subsequent isolation of a rare Ru $\eta^2$-benzaldehyde adduct likely boosts the reactivity of **1** in multicomponent reactions as well. Efforts to exploit this bonding motif in alternate catalytic transformations[43] are underway.

## ASSOCIATED CONTENT

### Supporting Information

The Supporting Information is available free of charge at https://pubs.acs.org/doi/10.1021/acs.organomet.0c00058.

Multinuclear NMR spectra and HR-MS spectra of all new compounds; details of optimization experiments and intermediate identification; crystallographic information file containing X-ray data with embedded structure factors and .res file (PDF)

### Accession Codes

CCDC 1978730−1978732 contain the supplementary crystallographic data for this paper. These data can be obtained free of charge via www.ccdc.cam.ac.uk/data_request/cif, or by emailing data_request@ccdc.cam.ac.uk, or by contacting The Cambridge Crystallographic Data Centre, 12 Union Road, Cambridge CB2 1EZ, UK; fax: +44 1223 336033.


https://dx.doi.org/10.1021/acs.organomet.0c00058
Organometallics XXXX, XXX, XXX−XXX

## AUTHOR INFORMATION


### Corresponding Author

**David E. Herbert** − *Department of Chemistry and the Manitoba Institute for Materials, University of Manitoba, Winnipeg, Manitoba R3T 2N2, Canada;* orcid.org/0000-0001-8190-2468; Email: david.herbert@umanitoba.ca

### Author

**Rajarshi Mondal** − *Department of Chemistry and the Manitoba Institute for Materials, University of Manitoba, Winnipeg, Manitoba R3T 2N2, Canada*

Complete contact information is available at: https://pubs.acs.org/10.1021/acs.organomet.0c00058


### Notes

The authors declare no competing financial interest.

## ACKNOWLEDGMENTS


The following sources of funding are gratefully acknowledged: Natural Sciences Engineering Research Council of Canada for a Discovery Grant to D.E.H. (RGPIN-2014-03733); the Canadian Foundation for Innovation and Research Manitoba for an award in support of an X-ray diffractometer (CFI #32146); and the University of Manitoba for GETS support (R.M.).


## REFERENCES


(1) Marco-Contelles, J.; Perez-Mayoral, E.; Samadi, A.; Carreiras, M.; Soriano, E. Recent Advances in the Friedlander Reaction. *Chem. Rev.* **2009**, *109*, 2652−2671.

(2) Martinez, R.; Ramon, D. J.; Yus, M. $RuCl_2(dmso)_4$ Catalyzes the Solvent-Free Indirect Friedlaender Synthesis of Polysubstituted Quinolines from Alcohols. *Eur. J. Org. Chem.* **2007**, *2007*, 1599−1605.

(3) Crabtree, R. H. Homogeneous Transition Metal Catalysis of Acceptorless Dehydrogenative Alcohol Oxidation: Applications in Hydrogen Storage and to Heterocycle Synthesis. *Chem. Rev.* **2017**, *117*, 9228−9246.

(4) Srimani, D.; Ben-David, Y.; Milstein, D. Direct Synthesis of Pyrroles by Dehydrogenative Coupling of β-Aminoalcohols With Secondary Alcohols Catalyzed by Ruthenium Pincer Complexes. *Angew. Chem., Int. Ed.* **2013**, *52*, 4012−4015.

(5) Srimani, D.; Ben-David, Y.; Milstein, D. Direct Synthesis of Pyridines and Quinolines by Coupling of γ-Amino-alcohols With Secondary Alcohols Liberating $H_2$ Catalyzed by Ruthenium Pincer Complexes. *Chem. Commun.* **2013**, *49*, 6632−6634.

(6) Pan, B.; Liu, B.; Yue, E.; Liu, Q.; Yang, X.; Wang, Z.; Sun, W.-H. A Ruthenium Catalyst with Unprecedented Effectiveness for the Coupling Cyclization of γ-Amino Alcohols and Secondary Alcohols. *ACS Catal.* **2016**, *6*, 1247−1253.

(7) Deng, D.; Hu, B.; Yang, M.; Chen, D. *NNN*-Ruthenium Catalysts for the Synthesis of Pyridines, Quinolines, and Pyrroles by Acceptorless Dehydrogenative Condensation. *Organometallics* **2018**, *37*, 2386−2394.

(8) Zhang, M.; Fang, X.; Neumann, H.; Beller, M. General and Regioselective Synthesis of Pyrroles via Ruthenium-Catalyzed Multicomponent Reactions. *J. Am. Chem. Soc.* **2013**, *135*, 11384−11388.

(9) Zhang, M.; Neumann, H.; Beller, M. Selective Ruthenium-Catalyzed Three-Component Synthesis of Pyrroles. *Angew. Chem., Int. Ed.* **2013**, *52*, 597−601.

(10) Kondo, T.; Yang, S.; Huh, K. T.; Kobayashi, M.; Kotachi, S.; Watanabe, Y. Ruthenium Complex-Catalyzed Facile Synthesis of 2-Substituted Benzoazoles. *Chem. Lett.* **1991**, *20*, 1275−8.

(11) Mastalir, M.; Glatz, M.; Pittenauer, E.; Allmaier, G.; Kirchner, K. Sustainable Synthesis of Quinolines and Pyrimidines Catalyzed by Manganese *PNP* Pincer Complexes. *J. Am. Chem. Soc.* **2016**, *138*, 15543−15546.

(12) Kallmeier, F.; Dudziec, B.; Irrgang, T.; Kempe, R. Manganese-Catalyzed Sustainable Synthesis of Pyrroles from Alcohols and Amino Alcohols. *Angew. Chem., Int. Ed.* **2017**, *56*, 7261−7265.

(13) Nguyen, D. H.; Trivelli, X.; Capet, F.; Paul, J.-F.; Dumeignil, F.; Gauvin, R. M. Manganese Pincer Complexes for the Base-Free, Acceptorless Dehydrogenative Coupling of Alcohols to Esters: Development, Scope, and Understanding. *ACS Catal.* **2017**, *7*, 2022−2032.

(14) Daw, P.; Kumar, A.; Espinosa-Jalapa, N. A.; Diskin-Posner, Y.; Ben-David, Y.; Milstein, D. Synthesis of Pyrazines and Quinoxalines via Acceptorless Dehydrogenative Coupling Routes Catalyzed by Manganese Pincer Complexes. *ACS Catal.* **2018**, *8*, 7734−7741.

(15) Ruch, S.; Irrgang, T.; Kempe, R. New Iridium Catalysts for the Selective Alkylation of Amines by Alcohols under Mild Conditions and for the Synthesis of Quinolines by Acceptor-less Dehydrogenative Condensation. *Chem. - Eur. J.* **2014**, *20*, 13279−13285.

(16) Deibl, N.; Ament, K.; Kempe, R. A Sustainable Multicomponent Pyrimidine Synthesis. *J. Am. Chem. Soc.* **2015**, *137*, 12804−12807.

(17) Hille, T.; Irrgang, T.; Kempe, R. Synthesis of meta-Functionalized Pyridines by Selective Dehydrogenative Heterocondensation of β- and γ-Amino Alcohols. *Angew. Chem., Int. Ed.* **2017**, *56*, 371−374.

(18) Midya, S. P.; Landge, V. G.; Sahoo, M. K.; Rana, J.; Balaraman, E. Cobalt-Catalyzed Acceptorless Dehydrogenative Coupling of Aminoalcohols With Alcohols: Direct Access to Pyrrole, Pyridine and Pyrazine Derivatives. *Chem. Commun.* **2018**, *54*, 90−93.

(19) Daw, P.; Chakraborty, S.; Garg, J. A.; Ben-David, Y.; Milstein, D. Direct Synthesis of Pyrroles by Dehydrogenative Coupling of Diols and Amines Catalyzed by Cobalt Pincer Complexes. *Angew. Chem., Int. Ed.* **2016**, *55*, 14373−14377.

(20) Shee, S.; Ganguli, K.; Jana, K.; Kundu, S. Cobalt Complex Catalyzed Atom-Economical Synthesis of Quinoxaline, Quinoline and 2-Alkylaminoquinoline Derivatives. *Chem. Commun.* **2018**, *54*, 6883−6886.

(21) Das, S.; Maiti, D.; De Sarkar, S. Synthesis of Polysubstituted Quinolines from α-2-Aminoaryl Alcohols Via Nickel-Catalyzed Dehydrogenative Coupling. *J. Org. Chem.* **2018**, *83*, 2309−2316.

(22) Chakraborty, G.; Sikari, R.; Das, S.; Mondal, R.; Sinha, S.; Banerjee, S.; Paul, N. D. Dehydrogenative Synthesis of Quinolines, 2-Aminoquinolines, and Quinazolines Using Singlet Diradical Ni(II)-Catalysts. *J. Org. Chem.* **2019**, *84*, 2626−2641.

(23) (a) Maji, M.; Kundu, S. Cooperative Ruthenium Complex Catalyzed Multicomponent Synthesis of Pyrimidines. *Dalton Trans.* **2019**, *48*, 17479−17487. (b) Maji, M.; Chakrabarti, K.; Paul, B.; Roy, B. C.; Kundu, S. Ruthenium(II)-NNN-Pincer-Complex-Catalyzed Reactions Between Various Alcohols and Amines for Sustainable C-N and C-C Bond Formation. *Adv. Synth. Catal.* **2018**, *360*, 722−729.

(24) Khusnutdinova, J. R.; Milstein, D. Metal-Ligand Cooperation. *Angew. Chem., Int. Ed.* **2015**, *54*, 12236−12273.

(25) Li, H.; Hall, M. B. Computational Mechanistic Studies on Reactions of Transition Metal Complexes with Noninnocent Pincer Ligands: Aromatization-Dearomatization or Not. *ACS Catal.* **2015**, *5*, 1895−1913.

(26) Gusev, D. G. Rethinking the Dehydrogenative Amide Synthesis. *ACS Catal.* **2017**, *7*, 6656−6662.

(27) Martinez, R.; Ramon, D. J.; Yus, M. $RuCl_2(dmso)_4$ Catalyzes the β-Alkylation of Secondary Alcohols with Primary Alcohols Through a Hydrogen Autotransfer Process. *Tetrahedron* **2006**, *62*, 8982−8987.

(28) (a) Cho, C. S.; Kim, B. T.; Choi, H.-J.; Kim, T.-J.; Shim, S. C. Ruthenium-Catalyzed Oxidative Coupling and Cyclization Between 2-Aminobenzyl Alcohol and Secondary Alcohols Leading to Quinolines. *Tetrahedron* **2003**, *59*, 7997−8002. (b) Cho, C. S.; Kim, B. T.; Kim, T.-J.; Shim, S. C. Ruthenium-catalyzed oxidative cyclization of 2-aminobenzyl alcohol with ketones: modified Friedlaender quinoline synthesis. *Chem. Commun.* **2001**, 2576−2577.

(29) Mondal, R.; Giesbrecht, P. K.; Herbert, D. E. Nickel(II), Copper(I) and Zinc(II) Complexes Supported by a (4-

Diphenylphosphino)phenanthridine Ligand. *Polyhedron* **2016**, *108*, 156−162.
(30) Feltham, R. D.; Metzger, H. G. The Synthesis of Vicinal Bis(dimethylarsino) Compounds. *J. Organomet. Chem.* **1971**, *33*, 347−355.
(31) Mandapati, P.; Giesbrecht, P. K.; Davis, R. L.; Herbert, D. E. Phenanthridine-Containing Pincer-like Amido Complexes of Nickel, Palladium, and Platinum. *Inorg. Chem.* **2017**, *56*, 3674−3685.
(32) Mondal, R.; Lozada, I. B.; Davis, R. L.; Williams, J. A. G.; Herbert, D. E. Site-Selective Benzannulation of *N*-Heterocycles in Bidentate Ligands Leads to Blue-Shifted Emission from $[(P\text{^}N)\text{-}Cu]_2(\mu\text{-}X)_2$ Dimers. *Inorg. Chem.* **2018**, *57*, 4966−4978.
(33) Lee, C.-I.; Zhou, J.; Ozerov, O. V. Catalytic Dehydrogenative Borylation of Terminal Alkynes by a SiNN Pincer Complex of Iridium. *J. Am. Chem. Soc.* **2013**, *135*, 3560−3566.
(34) Deibl, N.; Kempe, R. Manganese-Catalyzed Multicomponent Synthesis of Pyrimidines from Alcohols and Amidines. *Angew. Chem., Int. Ed.* **2017**, *56*, 1663−1666.
(35) Sultana Poly, S.; Siddiki, S. M. A. H.; Touchy, A. S.; Ting, K. W.; Toyao, T.; Maeno, Z.; Kanda, Y.; Shimizu, K.-i. Acceptorless Dehydrogenative Synthesis of Pyrimidines from Alcohols and Amidines Catalyzed by Supported Platinum Nanoparticles. *ACS Catal.* **2018**, *8*, 11330−11341.
(36) Robinson, S. D.; Levison, J. J. Transition-Metal Complexes Containing Phosphorus Ligands. III. Convenient Syntheses of Some Triphenylphosphine Complexes of the Platinum Metals. *J. Chem. Soc. A* **1970**, 2947−54.
(37) Romero, A.; Santos, A.; Lopez, J.; Echavarren, A. M. Reactions of $Ru(CO)ClH(C_5H_5N)(PPh_3)_2$ with 1-Alkynes. *J. Organomet. Chem.* **1990**, *391*, 219−23.
(38) Santos, A.; Lopez, J.; Galan, A.; Gonzalez, J. J.; Tinoco, P.; Echavarren, A. M. The Effect of *N*-Donor Ligands on the Reaction of Ruthenium Hydrides with 1-Alkynes. *Organometallics* **1997**, *16*, 3482−3488.
(39) Kühl, O. *Phosphorus-31 NMR Spectroscopy A Concise Introduction for the Synthetic Organic and Organometallic Chemist*; Springer: Berlin, Heidelberg, 2008.
(40) Roper, W. R.; Taylor, G. E.; Waters, J. M.; Wright, L. J. Dihapto-acyl Derivatives of Ruthenium(II). Preparation and Structure of $Ru[\eta^2\text{-}C(O)CH_3]I(CO)(PPh_3)_2$ and $Ru[\eta^2\text{-}C(O)p\text{-}tolyl]I(CO)\text{-}(PPh_3)_2$. *J. Organomet. Chem.* **1979**, *182*, C46−C48.
(41) Rodríguez-Lugo, R. E.; Trincado, M.; Vogt, M.; Tewes, F.; Santiso-Quinones, G.; Grützmacher, H. A Homogeneous Transition Metal Complex for Clean Hydrogen Production From Methanol-Water Mixtures. *Nat. Chem.* **2013**, *5*, 342.
(42) Anaby, A.; Schelwies, M.; Schwaben, J.; Rominger, F.; Hashmi, A. S. K.; Schaub, T. Study of Precatalyst Degradation Leading to the Discovery of a New $Ru^0$ Precatalyst for Hydrogenation and Dehydrogenation. *Organometallics* **2018**, *37*, 2193−2201.
(43) Hoshimoto, Y.; Ohashi, M.; Ogoshi, S. Catalytic Transformation of Aldehydes with Nickel Complexes through $\eta^2$ Coordination and Oxidative Cyclization. *Acc. Chem. Res.* **2015**, *48*, 1746−1755.


https://dx.doi.org/10.1021/acs.organomet.0c00058
*Organometallics* XXXX, XXX, XXX−XXX